HHS Public Access

Author manuscript

Ann Neurol. Author manuscript; available in PMC 2018 December 04.

Published in final edited form as:

Ann Neurol. 2017 December ; 82(6): 900–911. doi:10.1002/ana.25094.

A variant in *PPP4R3A* protects against Alzheimer-related metabolic decline

Leigh Christopher[1], **Valerio Napolioni**[1], **Raiyan R. Khan**[1], **Summer S. Han**[2], **Michael D. Greicius**[1], and **the Alzheimer's Disease Neuroimaging Initiative**

[1]Department of Neurology and Neurological Sciences, FIND Lab, Stanford University, Stanford, CA

[2]Quantitative Sciences Unit, Stanford Center for Biomedical Research (BMIR), Neurosurgery and Medicine, Stanford University

Abstract

Objectives—A reduction in glucose metabolism in the posterior cingulate cortex (PCC) predicts conversion to Alzheimer's disease (AD) and tracks disease progression, signifying its importance in AD. We aimed to use decline in PCC glucose metabolism as a proxy for the development and progression of AD to discover common genetic variants associated with disease vulnerability.

Methods—We performed a genome-wide association study (GWAS) of decline in PCC [^{18}F] FDG PET measured in Alzheimer's Disease Neuroimaging Initiative (ADNI) participants (n=606). We then performed follow-up analyses to assess the impact of significant single nucleotide polymorphisms (SNPs) on disease risk and longitudinal cognitive performance in a large independent dataset (n=870). Lastly, we assessed whether significant SNPs influence gene expression using two RNA sequencing (RNA-Seq) datasets (n=210 & n=159).

Results—We demonstrate a novel genome-wide significant association between rs2273647-T in the gene *PPP4R3A* and reduced [^{18}F] FDG decline (p= 4.44 × 10^{-8}). In a follow-up analysis using an independent dataset, we demonstrate a protective effect of this variant against risk of conversion to MCI or AD (p=0.038) and against cognitive decline in individuals who develop dementia (p = 3.41 × 10^{-15}). Furthermore, this variant is associated with altered gene expression in peripheral blood and altered *PPPP4R3A* transcript expression in temporal cortex, suggesting a role at the molecular level.

Correspondence should be addressed to Leigh Christopher, Department of Neurology & Neurological Sciences, FIND lab, Stanford University, 780 Welch Rd, Stanford, CA, lchris@stanford.edu.

*Data used in preparation of this article were obtained from the Alzheimer's Disease Neuroimaging Initiative (ADNI) database (adni.loni.usc.edu). As such, the investigators within the ADNI contributed to the design and implementation of ADNI and/or provided data but did not participate in analysis or writing of this report. A complete listing of ADNI investigators can be found at: http://adni.loni.usc.edu/wp-content/uploads/how_to_apply/ADNI_Acknowledgement_List.pdf

Author Contributions

L.C. and M.G. conceptualized and designed the study. L.C., V.N., R.K. & S.H. acquired and analyzed the data. L.C., V.N., R.K., S.H., & M.G. drafted the text and prepared figures.

Potential Conflicts of Interest

The authors declare no conflicts of interest.

Interpretations—*PPP4R3A* is a gene involved in AD risk and progression. Given the protective effect of this variant *PPP4R3A* should be further investigated as a gene of interest in neurodegenerative diseases and as a potential target for AD therapies.

Introduction

Among the many biomarkers for Alzheimer's disease (AD), decline in glucose metabolism in the posterior cingulate cortex (PCC) is one of the earliest, occurring years before symptom onset[1]. Furthermore, metabolic decline in the PCC actually predicts conversion from healthy aging to mild cognitive impairment (MCI), and from MCI to AD[2,3], signifying its role in AD progression. The PCC is a central and highly interconnected brain region, with a crucial role in coordinating memory and internally driven cognitive processes[4,5]. It is also a component of the default mode network (DMN), a brain network that is particularly vulnerable in AD[6,7]. Therefore, molecular pathways involved in declining PCC glucose metabolism may be closely associated with disease progression and worsening of symptoms. Although early decline in PCC glucose metabolism is well established in AD pathology, the genetic contribution to these changes remains unknown. Common genetic variation may influence the extent to which individuals are protected from or predisposed to hypometabolism, and as a result, their risk of developing AD and memory impairment. Genome-wide association studies (GWAS) have identified single nucleotide polymorphisms (SNPs), or common genetic variants, that are associated with hallmark pathological biomarkers of AD such as beta-amyloid plaques in the brain and phosphorylated tau in the CSF[8,9]. These studies have provided important insight into biological pathways associated with AD, however the link between PCC metabolic decline and vulnerability to AD is poorly understood. Decline in PCC metabolism correlates well with disease progression. By contrast, amyloid deposition measured with PET, appears less sensitive to disease progression[10,11]. As such, decline in PCC metabolism over time may provide distinct and important insights into biological mechanisms underlying the disease.

The primary aim of this study was to discover single nucleotide polymorphisms (SNPs) associated with longitudinal decline in PCC glucose metabolism that affect 1) the risk of developing AD and 2) the progression of the disease (i.e. cognitive decline). While the pathways linking PCC glucose metabolic decline to AD remain unknown, there is substantial evidence supporting a role for abnormal glucose regulation in AD. Cellular uptake of glucose is closely regulated by oxidative stress signaling pathways[12]. Furthermore, impaired oxidative stress signaling has been shown to lead to reduced glucose metabolism and the eventual development of memory impairment in AD[13]. Therefore, genes involved in adaptation to oxidative stress or the regulation of glucose metabolism may contribute to PCC metabolic decline and disease vulnerability. Since the PCC is the first and most pronounced region to undergo metabolic decline, PCC metabolism is a powerful and unexplored endophenotype for investigating unknown genetic contributions to AD. [^{18}F] FDG PET measures the uptake of glucose into neurons and astrocytes, and can be used as a proxy for neuronal activity. Thus, in order to achieve these aims we performed a quantitative trait GWAS of longitudinal decline in PCC glucose metabolism as measured by [^{18}F] FDG PET imaging in the Alzheimer's Disease Neuroimaging Initiative (ADNI) database. Our top

candidate from the GWAS was then explored further to determine its effects on AD risk, decline in cognitive performance over time, and gene expression in brain.

Methods

Participant Details

Participants included in the original imaging GWAS were part of the ADNI (http://www.adni.loni.usc.edu). We restricted the analysis to participants who were Caucasian with European ancestry. Individuals included in the imaging GWAS had [^{18}F] FDG PET data available at two time points at least a year apart. This included a total of 606 ADNI participants (mean age of 74 years ± 7.1 (standard deviation) mean education of 16 years ± 2.8, 43.7% *APOE**4 carriers and 37.8% female; Table 1). Participants for the analysis of conversion to MCI or AD and of longitudinal cognitive change were from the National Alzheimer's Coordinating Centre (NACC)[14-16]. This is a dataset including healthy elderly and AD participants with longitudinal clinical and cognitive data (Table 1). Participants for the brain RNA-Seq analysis were part of the MAYO RNA-Sequencing study[17] and the Rush Memory and Aging Project (MAP) [18]/Religious Orders Study (ROS)[19]. These are datasets with RNA-Seq transcript data and genotype data for healthy and AD participants. For the analysis of conversion to MCI or AD, we included healthy participants at baseline from NACC who had longitudinal clinical data and genotype data available (n= 870) in order to track their conversion over time (mean age of 74.9 years ± 8.8, mean education of 16 years ± 8.8, 28% *APOE**4 carriers and 59.2% female). For the longitudinal cognitive change analysis, we included all NACC participants who had longitudinal cognitive data at two time points at least a year apart and available genotype data (n= 851). All of the participants for this analysis overlapped with the participants included in the conversion analysis. For the RNA-Seq analysis we used two datasets from ROS/MAP and MAYO which provide RNA-Seq data from the dorsolateral prefrontal cortex and temporal cortex, respectively. For ROS/MAP we included all participants with available dorsolateral prefrontal cortex (DLPFC) RNA-Seq data and genotype data (n=220, mean age of death 84.4 ± 4.5, mean education of 16.7 ± 3.4, 25.9% *APOE**4 carriers and 66.4% female). For the MAYO dataset, we included all participants with available temporal cortex RNA-Seq data and genotype data (n= 159, mean age of death 80.3 ± 7.8, 32.9% *APOE**4 carriers and 55% female). All participants provided written informed consent and the protocols were approved by their respective review boards. NACC, ROS/MAP and MAYO study data were retrieved from the "NIA Genetics of Alzheimer's Disease Data Storage Site" (NIAGADS) and the Sage Bionetwork's Synapse project. The ADNI was launched in 2003 as a public-private partnership, led by Principal Investigator Michael W. Weiner, MD. The primary goal of ADNI has been to test whether serial magnetic resonance imaging, positron emission tomography, other biological markers, and clinical and neuropsychological assessment can be combined to measure the progression of mild cognitive impairment and early Alzheimer's disease. This was a re-analysis of de-identified data available from shared data repositories. Accession codes for the publicly available data used for the present study are reported in the Data Software and Availability Section. The study protocol was granted an exemption by the Stanford Institutional Review Board because the analyses were carried out on "de-identified, off-the-shelf" data.

Method Details

Imaging Analysis

All participants from ADNI-1 and ADNI-GO/2 with longitudinal [^{18}F] FDG-PET available were included in the GWAS. [^{18}F] FDG is used to measure resting cerebral metabolic rate of glucose uptake in the brain and is an early marker of neurodegeneration. [^{18}F] FDG-PET scans were acquired and pre-processed using a region of interest approach as described previously[20]. In brief, ROIs were created using a meta-analytic approach to determine regions most frequently associated with glucose metabolic changes and Alzheimer's disease. The PCC was selected as the primary ROI for this study. In previous work by Jagust et al., the most thoroughly pre-processed version of the ADNI [^{18}F] FDG-PET data were downloaded and uptake in each region of interest was normalized to uptake in the pons as a reference region, resulting in summary values of [^{18}F] FDG-PET uptake in a number of AD related brain regions[20]. These ROI data were used here to calculate decline in PCC [^{18}F] FDG as the mean annual percent decline from baseline between the first and last [^{18}F] FDG PET scan (Fig 1 A). Only participants who had at least one year of longitudinal follow-up were included.

Participants in NACC were used as an independent dataset to examine, respectively, the effect of significant SNPs obtained from the GWAS in ADNI on 1) risk of conversion to MCI or AD as assessed by the clinical diagnosis at each visit, 2) disease progression (i.e. longitudinal cognitive performance). RNA-Seq data from dorsolateral prefrontal cortex were also available for participants in the ROS and MAP studies and in participants from the MAYO study, and these were used to test the functional impact of significant SNPs on brain transcript expression levels.

Genotyping and Imputation

ADNI GWAS data were downloaded from the ADNI database. Genotyping in ADNI was performed using blood DNA samples with three genotyping arrays: Illumina 610-Quad, Illumina-OmniExpress or Illumina HumanOmni2.5-4v1 as previously described[21]. Genotype data underwent standard quality control including identity checks, cryptic relatedness (identity-by-descent (IBD) > 0.0625), sample exclusion for call rate< 95%, SNP exclusion for call rate< 95%, Hardy-Weinberg Equilibrium (HWE) of $p< 1 \times 10^{-6}$ and Minor Allele Frequency (MAF) < 1%. Unlinked SNPs [Linkage Disequilibrium (LD) pruning at r^2=0.1] passing the quality control criteria were used to determine the first ten principal components for population structure using EIGENSTRAT[22] and to remove population structure outliers. Imputation was performed using IMPUTE2 software, using the European population from the 1000 Genomes Project, Phase 3 as a reference panel[23]. After imputation, we excluded SNPs with an info quality score < 0.9, MAF < 0.05 and HWE ($p < 5 \times 10^{-6}$). This yielded a total of 2,820,932 SNPs for the GWAS analysis. A subset of ADNI subjects (n=818) was also whole-genome sequenced and available data were used to confirm the results obtained from SNP imputation. VCF files were annotated using SNPeff[24], and analyzed by PLINK 1.9[25]. GWAS data was also used for obtaining the genotype information for significant SNP(s) in our follow-up analyses. These datasets also underwent the same quality control pipeline and imputation described above.

Quantification and Statistical Analysis

GWAS—The GWAS was performed using PLINK software. The analysis was run using a linear regression under the assumption of an additive genetic model. Covariates included baseline age, sex, education, disease status and the first three principal components for population structure. We did not include *APOE**4 as a covariate in the initial GWAS, due to the colinearity between disease status and *APOE**4 dosage. The suggestive association threshold was $p < 1 \times 10^{-5}$ and the threshold for genome-wide significance was $p < 5 \times 10^{-8}$. This is a more conservative, consensus threshold for genome-wide significance based on correction for 1 million independent tests[26]. We aimed to discover SNPs passing the genome-wide significant threshold. Manhattan plots and QQ plots were generated using the package "qqman" in R (Version 3.3.1). Regional association plot was created using LocusZoom.

Competing Risks Regression Analysis

We ran a Competing Risks Regression analysis developed by Fine and Gray to evaluate the risk of conversion to MCI or AD by genotype (of significant SNPs), while accounting for death as a competing risk[27]. This analysis was carried out using the "cmprsk" package in R[28]. Competing risks analysis is a type of time-to-event analysis that aims to accurately estimate the marginal probability of an event in the presence of competing events such as death. This approach is relevant in this study because the participants are elderly and death may occur before the event of interest (i.e. conversion to MCI or AD) is observed, which can produce bias in risk estimates. We included all participants from the NACC dataset who were healthy at baseline, had genotyping data available, and had at least one year of follow-up to assess the effect of significant SNPs on risk of conversion. Age at entry, *APOE**4 status, sex and education were included as covariates in the analysis (n=870, Table 1). Disease was not included as a covariate as all participants were healthy at baseline.

Linear Mixed Effects Analysis of Longitudinal Cognition

We tested the association between significant SNPs and longitudinal change in cognitive performance using participants from the NACC dataset who had longitudinal neuropsychological testing data available (n=851). We used the Logical Memory Delayed Recall Score (out of 25) to assess episodic memory, the Boston Naming Task (BNT) (out of 30) to assess language and the Mini Mental State Examination (MMSE) (out of 30) to assess global cognitive function. These tests are known to be sensitive measures of cognitive decline in AD, and were acquired longitudinally in the NACC dataset. We tested all participants (n= 851) who were healthy at baseline who had available genotype information. We analyzed the data using a linear mixed effects model implemented in R, testing for the association between genotype and the change in cognitive performance over time i.e. a time by genotype interaction. This model accounts for correlations among repeated measurements within each participant, and permits varying observation periods and varying rates of decline among individuals. In addition to genotype, the time of measurement, and the interaction between these two variables, we included age at baseline, *APOE**4 dosage, final diagnosis, education and sex as covariates.

RNA-Seq Analysis

We tested whether transcript expression was altered between AD cases and controls for genes containing significant SNPs from the GWAS. We then tested the effect of significant SNPs on transcript expression of genes of interest using the ROS/MAP & MAYO RNA-Seq datasets from dorsolateral prefrontal cortex tissue and temporal cortex tissue, respectively. We used the general linear model implemented in R to perform a regression analysis looking at the effect of genotype on transcript expression for genes containing significant hits in the GWAS. All analyses included age at death, *APOE**4 status, sex, disease status, post-mortem interval (PMI) & education (not available in the MAYO dataset) as covariates. We removed outliers greater than 2 absolute standard deviations from the mean to exclude the possibility of sampling errors. We also examined two large publicly available online peripheral blood gene expression datasets to test whether significant SNPs modified gene expression in blood (https://eqtl.onderzoek.io/index.php?page=info & http://genenetwork.nl/bloodeqtlbrowser/).

Data and Software Availability

GWAS data and [^{18}F] FDG PET imaging data used in the present study were retrieved through ADNI (http://adni.loni.usc.edu). GWAS datasets for follow-up competing risks regression and linear mixed effects analyses were retrieved through NIAGADS (https://www.niagads.org) [ADC1 (NG00022), ADC2 (NG00023), ADC3 (NG00024)] for the NACC participants and [ROSMAP (NG00029)] for the ROS/MAP participants. Clinical and cognitive visit data for the NACC participants were obtained by request from the longitudinal uniform dataset (RDD-UDS). RNA-sequencing data in ROS/MAP participants and MAYO participants were obtained from Sage Bionetwork's Synapse project (https://www.synapse.org, syn3388564).

Results

GWAS identifies a variant in *PPP4R3A* associated with decline in PCC [^{18}F] FDG PET

There was a total of 606 ADNI participants included in the GWAS for PCC decline. Participants included a mixture of 192 healthy adults, 335 MCI patients and 79 AD patients.

We identified 130 SNPs that passed the suggestive association threshold (Fig 1 B, Supplementary Table 1). These SNPs corresponded to nine loci on 7 separate chromosomes. Only one SNP passed the genome-wide significance threshold (5×10^{-8}). This was rs2273647, an intronic variant located in the gene *PPP4R3A* (OMIM*610351, on chr. 14q32.12) (Fig 1 B, MAF= 0.326, $\beta = 1.303$, $p = 4.44 \times 10^{-8}$, Fig 2 A, Supplementary Table 1). The SNP, rs2273647 is located in a transcription factor binding site near a coding region of the gene *PPP4R3A* (alternate name *SMEK1).* One other SNP came close to genome-wide significance located on chromosome 10 in an intronic region of the gene *CDH23* (rs754726, β=−2.98, $p = 5.29 \times 10^{-8}$, See Supplementary Table 1). Rs2273647 in *PPP4R3A* was in high LD (r^2>0.8) with other SNPs located nearby on chromosome 14 (Fig 2 B). We generated a Q-Q plot to compare the observed versus the expected p values for the GWAS. The genomic inflation factor λ was equal to 1.00 indicating there is no systemic inflation of the observed p values in our dataset.

The minor allele of rs2273647-T demonstrated a protective effect on PCC glucose metabolic decline, with the homozygous minor allele group showing the least reduction in PCC glucose metabolism followed by the heterozygous group, and the homozygous wild-type groups (Fig 2 B). We determined that rs2273647 was an imputed SNP. Therefore, we checked the concordance rate between rs2273647 genotype in individuals who had whole genome sequencing data in ADNI. There was a 98% concordance rate between rs2273647 genotype and whole genome sequencing data in ADNI, confirming the validity of imputation for rs2273647.

There were 274 individuals who were homozygous wild-type (C/C), 266 individuals who were heterozygous (C/T) and 66 individuals who were homozygous recessive (T/T) at rs2273647 (Table 2). There were no significant differences in baseline age, education, sex or disease status between the three genotypes groups. There was a significant difference in the proportion of *APOE*4* carriers versus non-carriers ($p = 0.011$) across rs2273647 genotype groups. When the GWAS was rerun to include *APOE*4* status as a covariate in addition to the original covariates, the effect of rs2273647-T remains quite strong ($p = 1.67 \times 10^{-7}$).

PPP4R3A rs2273647-T Affects Risk of Conversion to MCI or AD

We aimed to assess whether the significant SNP was associated with risk of clinical conversion from healthy aging to MCI or AD. In order to evaluate the risk by genotype, we performed a competing risks regression analysis with death as the competing risk. Participants from the NACC dataset who were healthy controls at baseline, had longitudinal clinical visit data and had available genotype information were included in the analysis (Table 1, n =870). These subjects are independent from those used in the ADNI GWAS. For the 870 participants included in the analysis, the mean duration of follow-up was 4.3 years and the maximal follow-up time was 7 years. Risk of conversion was considered the risk of conversion from healthy to MCI or from healthy directly to AD (whichever conversion came first). Genotype was coded using an additive model (by dosage of the minor allele). Genotype for rs2273647 was significantly associated with risk of conversion to MCI or AD in 870 healthy controls. The minor allele (T) dosage was significantly associated with a reduced probability of developing MCI or AD (Fig 3 A, Hazard Ratio (HR)= 0.76, p= 0.038, n= 870). While the difference in risk between the heterozygote and homozygote T allele carriers was small, there was a more dramatic difference in the risk of conversion between the carriers and non-carriers of the T allele characteristic of a dominant effect. Therefore, we also ran the competing risks regression using a dominant model (ie. minor allele carriers (CT&TT) vs. non-carriers (CC)). There was a significant dominant effect on risk of conversion (Fig 3 B, HR= 0.70, p= 0.041, n= 870) with T allele carriers demonstrating a significantly lower risk compared to non-carriers.

To reduce the risk of bias due to the inclusion of individuals with a very short duration of follow-up, we restricted the analysis to those participants who had a minimum of 2 and 3 years of follow-up in separate analyses, and tested both the additive and dominant models. When we restricted the sample to those with a minimum of 2 years of follow-up (n=735, mean follow-up time of 4.8 years), there was a significant additive effect of genotype on risk of conversion (HR= 0.72, p=0.01, n=735) and an even stronger dominant effect on risk of

conversion (HR= 0.58, p=0.0014, n=735). When we restricted the sample to those with a minimum of 3 years of follow-up (n=635, mean follow-up time of 5.2 years), genotype was no longer significantly associated with risk of conversion for the additive model (p= 0.13), however, there was a strong significant association between genotype and risk of conversion for the dominant model (HR= 0.63, p= 0.006, n=635). These results suggest that genotype has a consistent and significant impact on the risk of developing disease. When comparing models, the dominant model provided a better model fit with lower Bayesian information criterion (BIC). Therefore, we used a dominant model as the default for the remainder of the follow-up analyses and reported additive model results as well.

PPP4R3A rs2273647-T Affects Longitudinal Cognitive Performance

Next, we aimed to assess the relationship between the *PPP4R3A* variant and cognitive performance over time. We performed a linear mixed effects analysis on all NACC participants to assess the association between rs2273647-T and the change in cognitive performance (memory, language and global cognition) over time, by evaluating time by rs2273647 interaction. All participants who were healthy at baseline had longitudinal cognitive data and genotype data available were included in the model and classified according to final diagnosis (n= 819 for BNT, n= 822 for MMSE & n= 854 for Logical Memory Delayed Recall). Our analysis showed that cognitive decline was modified by the genotype of rs2273647, with significant interaction for time by genotype observed on both BNT (p= 1.37×10^{-6}) and MMSE (p= 3.41×10^{-15}) in individuals with a final diagnosis of AD (Fig 4 A–B); the extent of cognitive decline over time was reduced among individuals with the T allele in rs2273647 versus wild type homozygotes, demonstrating its protective effect on cognitive performance. The results were also significant when using the additive model, for both the time by genotype effect on BNT ($p< 0.05$) and MMSE ($p< 5\times 10^{-6}$). All effects were significant after controlling for age at baseline, *APOE*4* dosage, final diagnosis, education and sex as covariates.

There were no significant time by genotype interactions in individuals with a final diagnosis of healthy or MCI, whose cognitive performance remained relatively stable over time (Fig 4 A–B). There were no significant interactions in any of the three groups on longitudinal logical memory (Fig 4 C).

PPP4R3A rs2273647-T Affects Gene Expression

Lastly, we wanted to assess whether *PPP4R3A* transcript expression is altered in disease and whether rs2273647-T has a functional impact on gene expression. First, we identified the most highly expressed transcripts in brain tissue for *PPP4R3A*. There were two transcripts that were fully annotated, protein coding and expressed in brain: ENST00000554684 & ENST00000555462. The mean expression in FPKM of ENST00000554684 in DLPFC and temporal cortex tissue was 1.41 (± 0.89) and 28.59 (± 5.34), respectively. The mean expression in FPKM of ENST00000555462 in DLPFC and temporal cortex was 1.39 (± 0.65) and 4.77 (± 0.98), respectively. Firstly, we aimed to test whether there were differences in the expression of *PPP4R3A* between AD cases and healthy controls in the RNA-Seq datasets from DLPFC and temporal cortex. We found a significant difference between cases and controls in ENST00000554684 expression after controlling for age at

death, sex, *APOE**4 status and PMI. The healthy controls demonstrated lower expression compared to AD (Fig 5 B, $p = 0.0038$, $n = 159$), suggesting that transcript expression of this gene is altered by disease. There were no significant differences between AD and healthy controls within DLPFC tissue for either transcript.

Next, we aimed to assess whether rs2273647 genotype is associated with altered transcript expression. The rs2273647-T genotype was associated with lower *PPP4R3A* ENST00000555462 transcript expression in temporal cortex of healthy control participants from the MAYO dataset, with carriers of the minor allele demonstrating lower transcript expression compared to non-carriers (Fig 5 A, $p = 0.011$, $n = 159$). Our results were also significant when using an additive model ($p = 0.015$). There was no significant difference in expression of this isoform in AD participants. Furthermore, there was no effect of genotype on transcript expression in the DLPFC tissue from the ROS/MAP dataset.

Finally, we took advantage of two, large web-based expression quantitative trait loci (eQTL) datasets to test the effect of rs2273647-T dose on *PPP4R3A* expression in peripheral blood. Results in these datasets are only available for the additive model. We found that rs2273647 was an eQTL, lowering the expression of *PPP4R3A* in blood with increasing dosage of the minor allele in a large meta-analysis of 9 datasets including 5311 samples ($p = 4.75 \times 10^{-10}$, $Z = -6.23$)[29]. We were able to confirm this result in a second blood eQTL dataset of 4896 participants of European ancestry ($p = 2.53 \times 10^{-10}$; https://eqtl.onderzoek.io), providing further support for the involvement of this variant in modifying gene expression in blood[30].

Discussion

Previous GWAS studies using imaging markers including hippocampal atrophy, beta-amyloid, and CSF tau have provided insight into the mechanisms underlying genetic vulnerability to AD, implicating a number of genes associated with these AD endophenotypes[8,9,21,31]. The significant advantage of using PCC metabolic decline as an endophenotype in the present study, is that it is a consistent early biomarker for AD that has been shown to correlate well with disease progression, to a greater extent than beta-amyloid deposition[10,11]. Thus, using it as an endophenotype has the potential to reveal important genes that are closely associated with the mitigation (or exacerbation) of disease progression.

In this study, we demonstrate that rs2273647-T is associated with less metabolic decline in the PCC, a reduced risk of conversion to MCI or AD and reduced cognitive decline. Previous studies have tested for associations between known AD risk variants and imaging markers of AD progression including PCC hypometabolism[32], however, this is the first study to identify a novel genome-wide association between a common variant and longitudinal PCC metabolic decline.

Taken together, these results suggest that the T allele confers a protective advantage by preserving brain glucose uptake in the face of AD pathology. We show that rs2273647-T is associated with a reduced risk of conversion to MCI or AD, suggesting that *PPP4R3A* plays a role in predisposition to disease. We also show that rs2273647-T is protective against

language and global cognitive decline, in those individuals who progress to AD over their follow-up period. The lack of significant interaction effects in those who remain healthy or convert to MCI in our study is likely due to the fact that many of these participants remained healthy for a large proportion of the study and do not show substantial decline regardless of genotype (as is apparent in Fig 4), thus obscuring the effect of rs2273647-T. Our findings demonstrate a strong protective effect in those individuals who convert to AD, especially against global cognitive decline, emphasizing that individuals carrying rs2273647-T perform better despite the onset of disease.

In order to provide a functional link between *PPP4R3A* at the molecular level and the clinical level, we aimed to assess whether rs2273647 genotype was significantly associated with *PPP4R3A* transcript expression. We were able to detect a significant effect of genotype in healthy controls for one of the protein-coding transcripts in temporal cortex, whereby healthy control carriers demonstrated lower transcript expression. We also demonstrated that transcript expression is significantly lower in healthy controls compared to AD, providing further evidence that *PPP4R3A* is altered in disease. The reason for healthy control carriers demonstrating lower transcript expression, but not AD participants is unclear, however, it is possible that the effect of disease on transcript expression outweighs the effect of the protective genotype. The lack of replication of these results in the DLPFC may be due to a regional effect of rs2276347 on transcript expression within the temporal cortex, which is more strongly affected by AD progression. Gene expression changes appear to be triggered by the onset of AD-associated pathology, which is present earlier and to a greater extent in the temporal cortex than in the frontal cortex. Further work will be needed to determine the regionally specific effects of rs2273647 on gene expression in the brain.

In previous work *PPP4R3A* was shown to be involved in gluconeogenesis. Furthermore, reduced expression of *PPP4R3A* was directly linked to lower fasting blood glucose levels, while increased *PPP4R3A* expression was linked to insulin resistance[33]. This strongly suggests that *PPP4R3A* plays an important role in influencing glucose uptake in humans, and that increased *PPP4R3A* expression may be detrimental. More tellingly, the SNP identified here has been associated with reduced fasting blood glucose levels ($\beta = -0.015$, $p = 1.7 \times 10^{-4}$)[34]. Furthermore, we confirmed that it is an eQTL in blood in two independent datasets, significantly reducing gene expression in T allele carriers[29,30]. Taking this into consideration with our findings, rs2273647-T carriers may have reduced gene expression and reduced fasting blood glucose levels, which could contribute directly to a protective effect on [^{18}F] FDG decline. Conversely, higher expression of *PPP4R3A* may result in insulin resistance and reduced brain glucose uptake, which has been linked to AD[12,35]. Another possibility, is that T-allele carriers experience a lower risk for diabetes as a result of their differential glucose regulation, thus indirectly affecting AD risk and brain metabolic decline[36]. Reduced brain glucose uptake is an early marker of neurodegeneration, and not necessarily specific to AD. Therefore, it is possible that *PPP4R3A* may influence vulnerability to multiple neurodegenerative diseases[37]. Although the exact mechanism of action of *PPP4R3A* in AD is unknown, abnormal regulation of insulin signaling and glucose metabolism is associated with greater oxidative stress, and thus *PPP4R3A* may play a role in the predisposition of neuronal cells to oxidative damage and metabolic dysfunction associated with neurodegenerative disease pathology. Interestingly, *smk-1* (*PPP4R3A*

ortholog) has been shown to play a direct role in mediating longevity via the insulin-signaling pathway[38,39]. Furthermore, accumulating evidence suggests that the effective regulation of insulin-signaling promotes healthy aging and is protective against toxic age-related protein aggregation including amyloid-beta[40–42]. Thus, alterations in *PPP4R3A* may help slow the onset and accumulation of AD pathology via the modification of insulin-signaling pathways. In a follow-up search for previous associations between *PPP4R3A* and AD risk, we found that a distinct variant in *PPP4R3A* passed the suggestive threshold for association with risk of AD in a family-based GWAS, lending additional support for the involvement of this gene in AD[43]. Further investigations will be needed to identify the protective mechanisms by which *PPP4R3A* affects disease vulnerability.

One limitation to our study is that we have not been able to determine definitively whether the true biological effect of rs2273647-T is dominant or additive. As is conventionally done in GWAS studies, we identified this variant in our initial analysis with an additive model. We observed in the follow-up analyses, however, the effect of genotype on disease risk, progression, and gene expression was stronger when rs2273647 genotype was classified according to a dominant model. We therefore returned to the original GWAS and checked the p-value of our SNP assuming a dominant model and found that it remains quite significant at $p = 1.32 \times 10^{-7}$. On balance, our results support an additive model with the dominant model appearing stronger mainly in those analyses (such as gene expression in brain) with smaller sample sizes and relatively few homozygous recessive subjects.

In conclusion, we identify a novel protective variant in the gene *PPP4R3A* associated with reduced glucose metabolic decline. We were able to replicate the protective effect in an independent dataset, demonstrating that the minor allele at rs2273647 is associated with a reduced risk of developing AD and a slower rate of cognitive decline in subjects who ultimately develop AD. Importantly, our findings strongly support a role for *PPP4R3A* in AD vulnerability and progression. Furthermore, this variant affects *PPP4R3A* gene expression indicating a functional effect. While the specific biological pathways underlying the role of *PPP4R3A* in AD vulnerability require further investigation, the results reported here suggest that *PPP4R3A* should be considered as a potential therapeutic target in AD.

Supplementary Material

Refer to Web version on PubMed Central for supplementary material.

Acknowledgments

CIHR Fellowship Award, NIH:P50 AG047366, McKnight Memory and Cognitive Disorders Award, Feldman Foundation CA, The JNA Foundation, The J. W. Bagley Foundation, and The Mervin and Roslyn Morris Educational and Philanthropic Fund.

Data collection and sharing for this project was funded by the Alzheimer's Disease Neuroimaging Initiative (ADNI) (National Institutes of Health Grant U01 AG024904) and DOD ADNI (Department of Defense award number W81XWH-12-2-0012). ADNI is funded by the National Institute on Aging, the National Institute of Biomedical Imaging and Bioengineering, and through generous contributions from the following: AbbVie, Alzheimer's Association; Alzheimer's Drug Discovery Foundation; Araclon Biotech; BioClinica, Inc.; Biogen; Bristol-Myers Squibb Company; CereSpir, Inc.; Cogstate; Eisai Inc.; Elan Pharmaceuticals, Inc.; Eli Lilly and Company; EuroImmun; F. Hoffmann-La Roche Ltd and its affiliated company Genentech, Inc.; Fujirebio; GE Healthcare; IXICO Ltd.; Janssen Alzheimer Immunotherapy Research & Development, LLC.; Johnson & Johnson

Pharmaceutical Research & Development LLC.; Lumosity; Lundbeck; Merck & Co., Inc.; Meso Scale Diagnostics, LLC.; NeuroRx Research; Neurotrack Technologies; Novartis Pharmaceuticals Corporation; Pfizer Inc.; Piramal Imaging; Servier; Takeda Pharmaceutical Company; and Transition Therapeutics. The Canadian Institutes of Health Research is providing funds to support ADNI clinical sites in Canada. Private sector contributions are facilitated by the Foundation for the National Institutes of Health (www.fnih.org). The grantee organization is the Northern California Institute for Research and Education, and the study is coordinated by the Alzheimer's Therapeutic Research Institute at the University of Southern California. ADNI data are disseminated by the Laboratory for Neuro Imaging at the University of Southern California.

References

1. Minoshima S, Giordani B, Berent S, et al. Metabolic reduction in the posterior cingulate cortex in very early Alzheimer's disease. Ann Neurol. 1997; 42(1):85–94. [PubMed: 9225689]
2. de Leon MJ, Convit A, Wolf OT, et al. Prediction of cognitive decline in normal elderly subjects with 2-[(18)F]fluoro-2-deoxy-D-glucose/poitron-emission tomography (FDG/PET). Proc Natl Acad Sci. 2001; 98(19):10966–71. [PubMed: 11526211]
3. Chételat G, Desgranges B, de la Sayette V, et al. Mild cognitive impairment: Can FDG-PET predict who is to rapidly convert to Alzheimer's disease? Neurology. 2003; 60:1374–1377. [PubMed: 12707450]
4. Fransson P, Marrelec G. The precuneus/posterior cingulate cortex plays a pivotal role in the default mode network: Evidence from a partial correlation network analysis. Neuroimage. 2008; 42(3): 1178–1184. [PubMed: 18598773]
5. Leech R, Sharp DJ. The role of the posterior cingulate cortex in cognition and disease. Brain. 2014; 137(1):12–32. [PubMed: 23869106]
6. Buckner RL, Andrews-Hanna JR, Schacter DL. The brain's default network: anatomy, function, and relevance to disease. Ann N Y Acad Sci. 2008; 1124:1–38. [PubMed: 18400922]
7. Greicius MD, Srivastava G, Reiss AL, Menon V. Default-mode network activity distinguishes Alzheimer's disease from healthy aging: evidence from functional MRI. Proc Natl Acad Sci. 2004; 101(13):4637–42. [PubMed: 15070770]
8. Cruchaga C, Kauwe JSK, Harari O, et al. GWAS of Cerebrospinal Fluid Tau Levels Identifies Risk Variants for Alzheimer's Disease. Neuron. 2013; 78(2):256–268. [PubMed: 23562540]
9. Ramanan VK, Risacher SL, Nho K, et al. GWAS of longitudinal amyloid accumulation on 18F-florbetapir PET in Alzheimer's disease implicates microglial activation gene IL1RAP. Brain. 2015; 138(10):3076–3088. [PubMed: 26268530]
10. Engler H, Forsberg A, Almkvist O, et al. Two-year follow-up of amyloid deposition in patients with Alzheimer's disease. Brain. 2006; 129:2856–2866. [PubMed: 16854944]
11. Kadir A, Almkvist O, Forsberg A, et al. Dynamic changes in PET amyloid and FDG imaging at different stages of Alzheimer's disease. Neurobiol Aging. 2012; 33:198.e1–198.e14.
12. Sabio G, Das M, Mora A, et al. A stress signaling pathway in adipose tissue regulated hepatic insulin resistance. Science. 2008; 322(5907):1539–1543. [PubMed: 19056984]
13. Westwood AJ, Beiser A, DeCarli C, et al. Insulin-like growth factor-1 and risk of Alzheimer dementia and brain atrophy. Neurology. 2014; 82(18):1613–1619. [PubMed: 24706014]
14. Weintraub S, Salmon D, Mercaldo N, et al. The Alzheimer's disease centers' data set (UDS): The neuropsychological test battery. Alzheimer Dis Assoc Disord. 2009; 23(2):91–101. [PubMed: 19474567]
15. Morris JC, Weintraub S, Chui HC, et al. The Uniform Data Set (UDS): Clinical and Cognitive Variables and Descriptive Data From Alzheimer Disease Centers. Alzheimer Dis Assoc Disord. 2006; 20(4):210–216. [PubMed: 17132964]
16. Beekly DL, Ramos EM, Lee WW, et al. The National Alzheimer's Coordinating Center (NACC) database: the Uniform Data Set. Alzheimer Dis Assoc Disord. 2007; 21(3):249–258. [PubMed: 17804958]
17. Allen M, Carrasquillo MM, Funk C, et al. Human whole genome genotype and transcriptome data for Alzheimer's and other neurodegenerative diseases. Sci data. 2016; 3:160089. [PubMed: 27727239]

18. Bennett DA, Schneider JA, Buchman AS, et al. Overview and findings from the rush Memory and Aging Project. Curr Alzheimer Res. 2012; 9(6):646–663. [PubMed: 22471867]
19. Bennett DA, Schneider JA, Arvanitakis Z, et al. Overview and findings from the religious orders study. Curr Alzheimer Res. 2012; 9(6):628–645. [PubMed: 22471860]
20. Jagust WJ, Bandy D, Chen K, et al. The Alzheimer's Disease Neuroimaging Initiative positron emission tomography core. Alzheimer's Dement. 2010; 6(3):221–229. [PubMed: 20451870]
21. Saykin AJ, Shen L, Foroud TM, et al. Alzheimer's Disease Neuroimaging Initiative biomarkers as quantitative phenotypes: Genetics core aims, progress, and plans. Alzheimer's Dement. 2010; 6(3): 265–273. [PubMed: 20451875]
22. Price AL, Patterson NJ, Plenge RM, et al. Principal components analysis corrects for stratification in genome-wide association studies. Nat Genet. 2006; 38(8):904–909. [PubMed: 16862161]
23. Auton A, Abecasis GR, Altshuler DM, et al. A global reference for human genetic variation. Nature. 2015; 526(7571):68–74. [PubMed: 26432245]
24. Cingolani P, Platts A, Wang LL, et al. A program for annotating and predicting the effects of single nucleotide polymorphisms, SnpEff: SNPs in the genome of Drosophila melanogaster strain w 1118; iso-2; iso-3. Fly. 2012; 6(2):80–92. [PubMed: 22728672]
25. Chang CC, Chow CC, Tellier LC, et al. Second-generation PLINK: rising to the challenge of larger and richer datasets. Gigascience. 2015; 4(1):7. [PubMed: 25722852]
26. Risch N, Merikangas K. The Future of Genetic Studies of Complex Human Diseases. Science. 1996; 273(5281):1516–1517. [PubMed: 8801636]
27. Fine JP, Gray RJ, Fine JP, Gray RJ. A Proportional Hazards Model for the Subdistribution of a Competing Risk. J Am Stat Assoc. 1999; 94(446):496–509.
28. Scrucca L, Santucci A, Aversa F. Regression modeling of competing risk using R: an in depth guide for clinicians. Bone Marrow Transplant. 2010; 45(9):1388–1395. [PubMed: 20062101]
29. Westra H-J, Peters MJ, Esko T, et al. Systematic identification of trans eQTLs as putative drivers of known disease associations. Nat Genet. 2013; 45(10):1238–43. [PubMed: 24013639]
30. Jansen R, Hottenga JJ, Nivard MG, et al. Conditional eQTL analysis reveals allelic heterogeneity of gene expression. Hum Mol Genet. 2017; 26(8):1444–1451. [PubMed: 28165122]
31. Potkin SG, Guffanti G, Lakatos A, et al. Hippocampal atrophy as a quantitative trait in a genome-wide association study identifying novel susceptibility genes for Alzheimer's Disease. PLoS One. 2009; 4(8)
32. Stage E, Duran T, Risacher SL, et al. The effect of the top 20 Alzheimer disease risk genes on gray-matter density and FDG PET brain metabolism. Alzheimer's Dement (Amst). 2016; 5:53–66. [PubMed: 28054028]
33. Yoon Y-S, Lee M-W, Ryu D, et al. Suppressor of MEK null (SMEK)/protein phosphatase 4 catalytic subunit (PP4C) is a key regulator of hepatic gluconeogenesis. Proc Natl Acad Sci. 2010; 107(41):17704–9. [PubMed: 20876121]
34. Dupuis J, Langenberg C, Prokopenko I, et al. New genetic loci implicated in fasting glucose homeostasis and their impact on type 2 diabetes risk. Nat Genet. 2010; 42(2):105–16. [PubMed: 20081858]
35. Craft S. Insulin resistance syndrome and Alzheimer's disease: Age- and obesity-related effects on memory, amyloid, and inflammation. Neurobiol Aging. 2005; 26(SUPPL 1):65–69. [PubMed: 16266773]
36. Baker LD, Cross DJ, Minoshima S, et al. Insulin resistance and Alzheimer-like reductions in regional cerebral glucose metabolism for cognitively normal adults with prediabetes or early type 2 diabetes. Arch Neurol. 2011; 68(1):51–57. [PubMed: 20837822]
37. Mosconi L, Tsui WH, Herholz K, et al. Multicenter standardized 18F-FDG PET diagnosis of mild cognitive impairment, Alzheimer's disease, and other dementias. J Nucl Med. 2008; 49(3):390–8. [PubMed: 18287270]
38. Wolff S, Ma H, Burch D, et al. SMK-1, an essential regulator of DAF-16-mediated longevity. Cell. 2006; 124(5):1039–1053. [PubMed: 16530049]
39. Libina N, Berman JR, Kenyon C. Tissue-Specific Activities of C. elegans DAF-16 in the Regulation of Lifespan. Cell. 2003; 115(4):489–502. [PubMed: 14622602]

40. Cohen E, Dillin A. The insulin paradox: aging, proteotoxicity and neurodegeneration. Nat Rev Neurosci. 2008; 9(10):759–767. [PubMed: 18769445]

41. De Felice FG, Vieira MNN, Bomfim TR, et al. Protection of synapses against Alzheimer's-linked toxins: insulin signaling prevents the pathogenic binding of Abeta oligomers. Proc Natl Acad Sci. 2009; 106(6):1971–6. [PubMed: 19188609]

42. Carro E, Trejo JL, Gerber A, et al. Therapeutic actions of insulin-like growth factor I on APP/PS2 mice with severe brain amyloidosis. Neurobiol Aging. 2006; 27(9):1250–1257. [PubMed: 16183170]

43. Herold C, Hooli BV, Mullin K, et al. Family-based association analyses of imputed genotypes reveal genome-wide significant association of Alzheimer's disease with OSBPL6, PTPRG, and PDCL3. Mol Psychiatry. 2016; 21(11):1608–1612. [PubMed: 26830138]

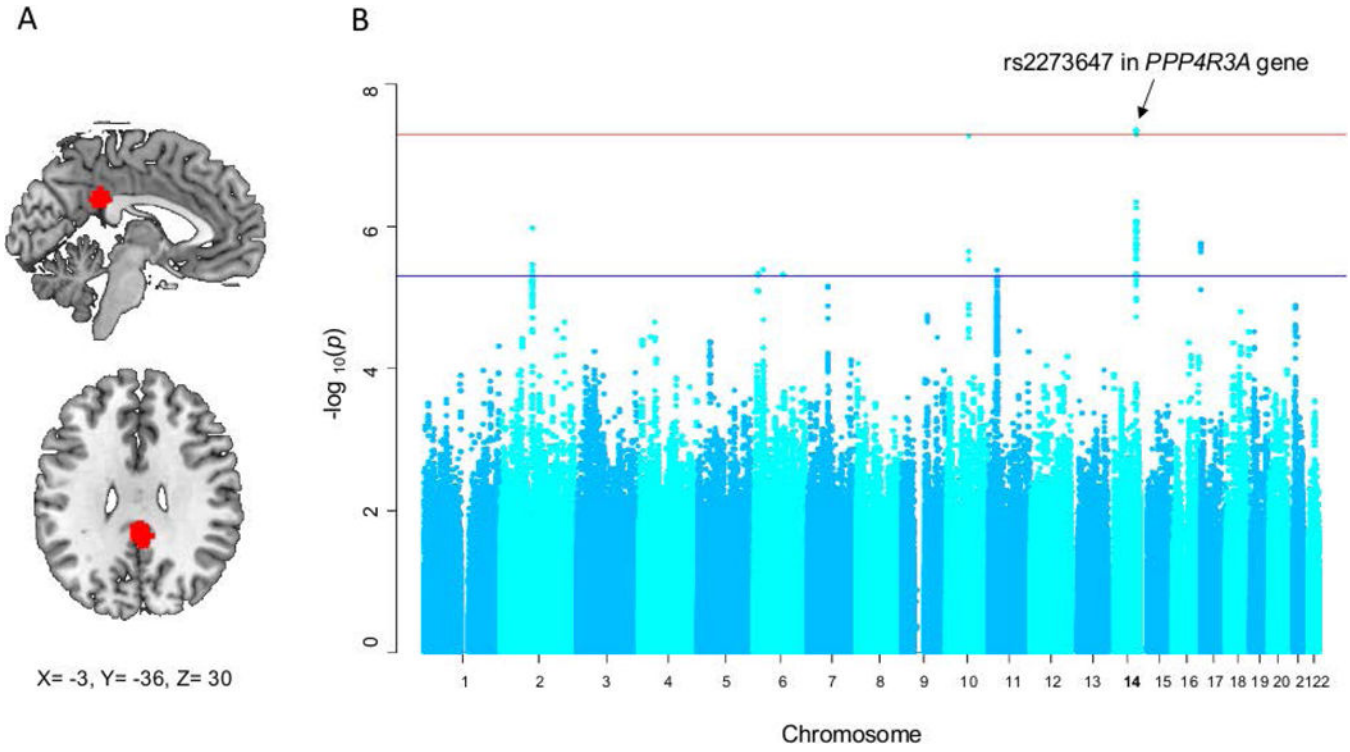

Figure 1.

A common variant in *PPP4R3A* is associated with less decline in posterior cingulate glucose metabolism. **A.** PCC ROI overlaid on a template brain in MNI space illustrating the region where [^{18}F] FDG PET decline was measured for each participant. MNI coordinates are displayed below. B. Manhattan plot demonstrating the results of the GWAS including all ADNI participants. The blue line represents a suggestive association threshold (1×10^{-5}) and the red line indicates the genome-wide association threshold (5×10^{-8}). Arrow indicates significant SNP passing genome-wide significance threshold located on Chromosome 14 in an intronic region of the *PPP4R3A* gene.

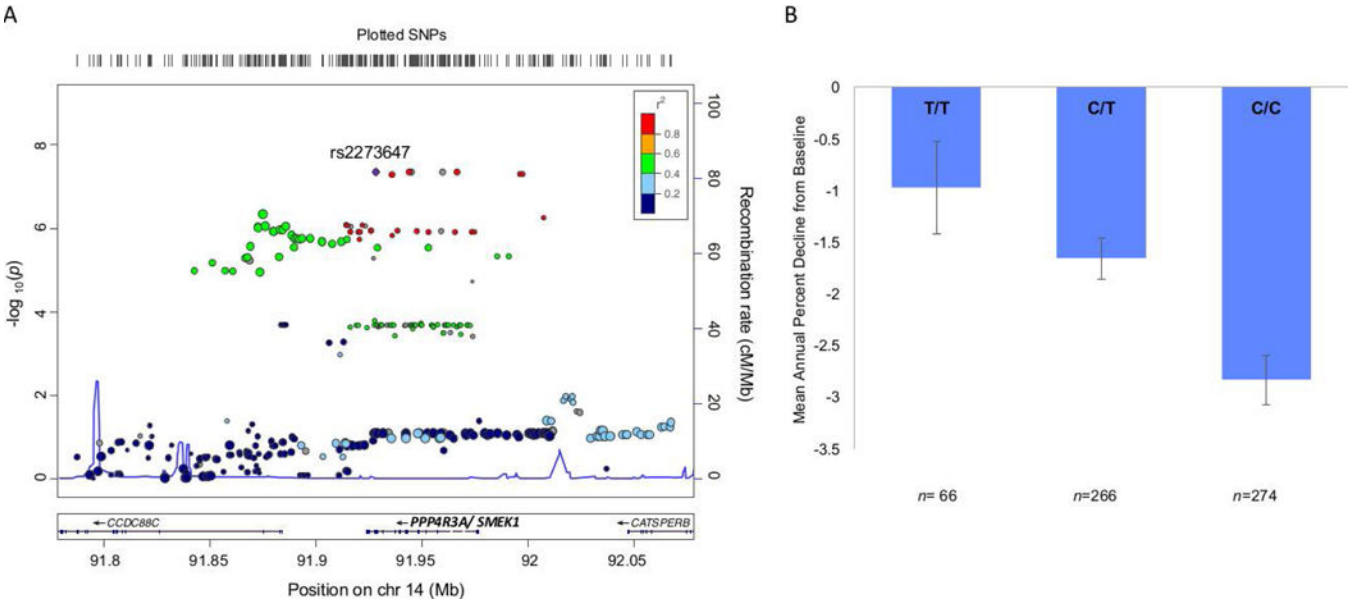

Figure 2.

Regional association and pattern of PCC [^{18}F] FDG decline for rs2273647 in *PPP4R3A*. **A.** Regional association plot demonstrating regional linkage disequilibrium for rs2273647 with other SNPs. **B.** Longitudinal decline in PCC glucose metabolism by rs2273647 genotype. The T allele is associated with significantly less decline in glucose metabolism.

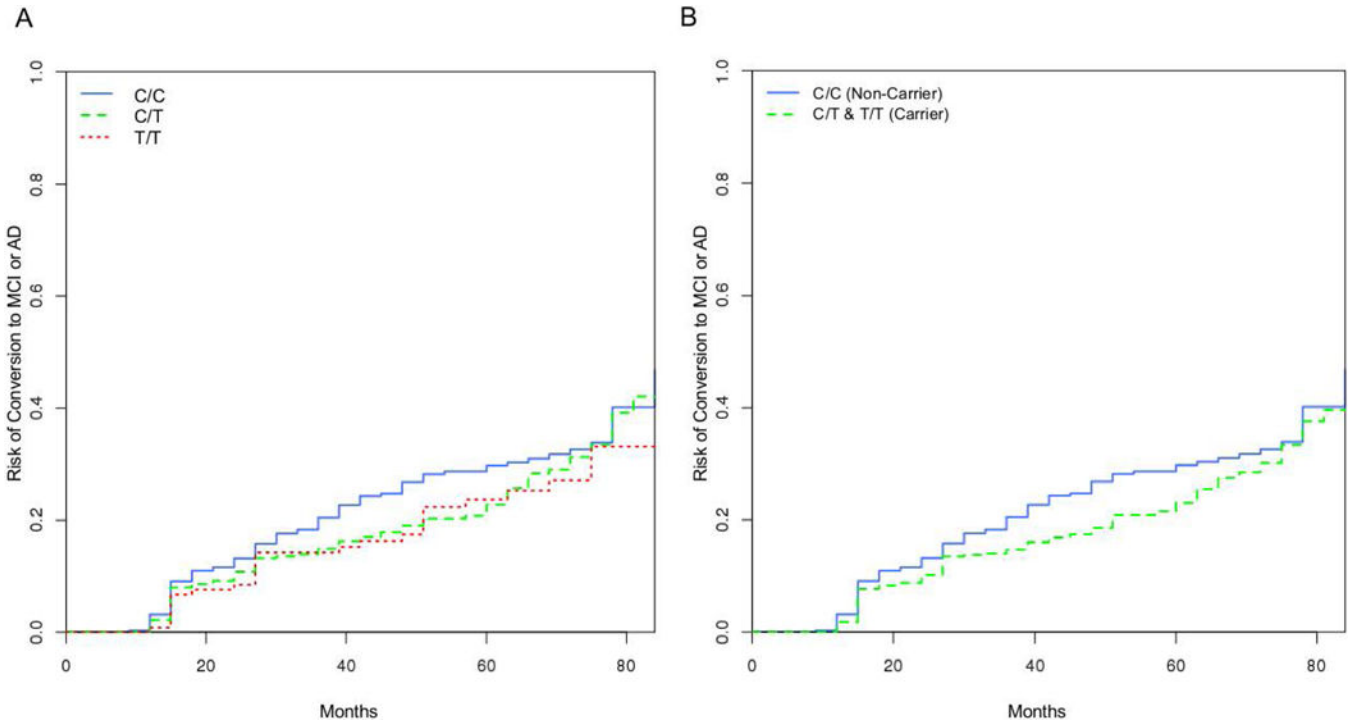

Figure 3.

The minor allele (T) of rs2273647 in *PPP4R3A* is associated with reduced risk of conversion to MCI or AD. A. Cumulative incidence functions demonstrating the risk of conversion to MCI or AD for three genotypes of rs2273647 over a 7-year time period using an additive model. T allele dosage was significantly associated with the risk of conversion to MCI or AD over time after controlling for *APOE**4 status, age at entry, sex and education (HR = 0.76, p= 0.038, n=870). **B.** Cumulative incidence functions demonstrating the risk of conversion to MCI or AD using a dominant model. T allele carriers demonstrate significantly lower risk of conversion to MCI or AD over time after controlling for *APOE**4 status, age at entry, sex and education (HR = 0.70, p= 0.041, n=870).

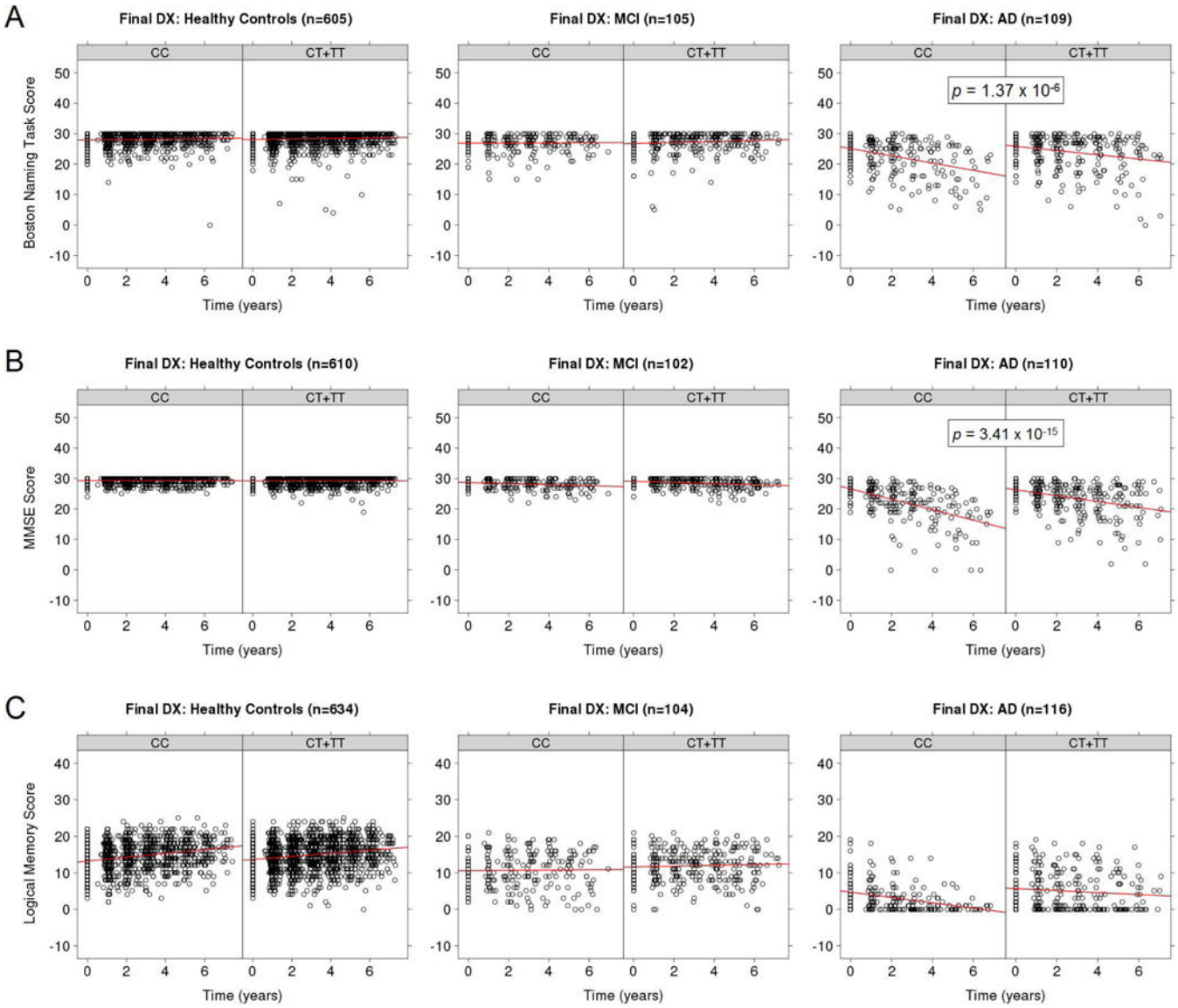

Figure 4.

Cognitive decline is significantly modified by genotype in individuals with a final diagnosis of AD. A. Participants who develop AD demonstrate a significant time by genotype interaction on BNT scores ($p = 1.37 \times 10^{-6}$, $n = 819$) indicating a protective effect on language decline. B. Participants who develop AD demonstrate a significant time by genotype interaction on MMSE scores ($p = 3.41 \times 10^{-15}$, $n = 822$) indicating a protective effect on global cognitive decline. Interactions were significant after controlling for baseline age, education, *APOE**4 dosage and sex. C. Time by genotype effect was not significant for longitudinal memory scores in any diagnostic category. Final DX = Final diagnosis.

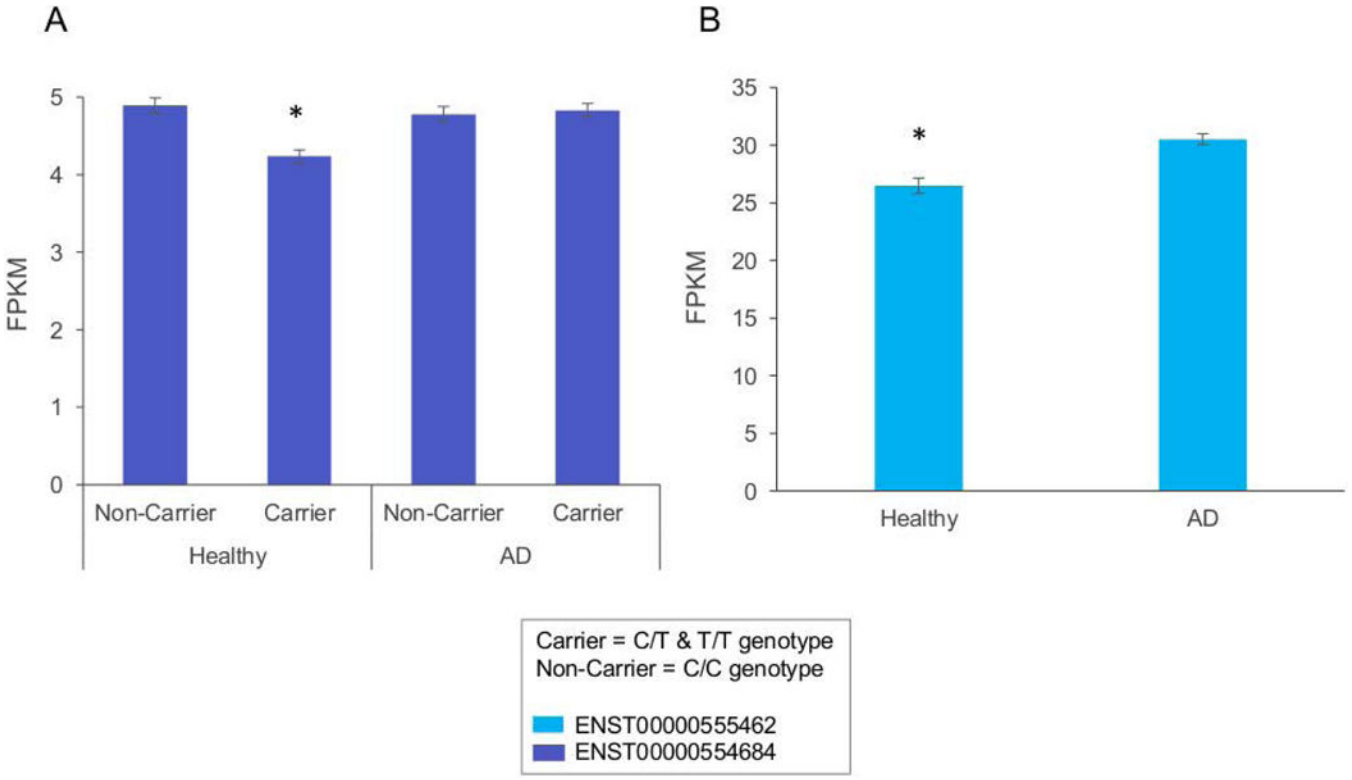

Figure 5. The effect of genotype and disease status on *PPP4R3A* transcript expression. A There is a significant dominant effect of genotype on transcript expression (ENST00000555462) in the temporal cortex of healthy controls with T allele carriers demonstrating lower expression compared to non-carriers (p= 0.011, n= 159). There is no significant effect of genotype on transcript expression in AD. **B.** *PPP4R3A* transcript expression (ENST00000554684) is significantly lower in healthy control compared to Alzheimer's disease patients in temporal cortex (p=0.0038, n= 149). FPKM = Fragments Per Kilobase of transcript per Million mapped reads.

Table 1

Participant Demographics

Table demonstrates demographics for each dataset used in the GWAS (ADNI) and follow-up analyses including the analysis for conversion to MCI or AD (NACC) & the analysis for longitudinal cognition (NACC). Values in brackets are standard deviation. ADNI= Alzheimer's Disease Neuroimaging Initiative; NACC= National Alzheimer's Coordinating Centre.

	ADNI	NACC
Participants (*n*)	606	870
*APOE**4 (Carriers/Non-Carriers)	265/341	244/626
Baseline Age (years)	74.1 (7.1)	74.9 (8.80.30)
Education (years)	16.0 (2.8)	16.8 (8.80.94)
Sex (Female/Male)	229/377	515/355

Table 2

RNA-Seq Participant Demographics

Table demonstrates demographic information for each dataset used in the RNA-Seq analysis. Values in brackets are standard deviation. MCI = Mild Cognitive Impairment, AD = Alzheimer's Disease, DPLFC = Dorsolateral Prefrontal Cortex, BA = Broadmann Area

	ROS/MAP RNA-Seq	MAYO RNA-Seq
Participants (n)	220	149
*APOE**4 (Carriers/Non-Carriers)	57/163	49/100
Age at Death (years)	84.4 (4.5)	80.3 (7.8)
Sex (Female/Male)	146/74	82/67
Disease Group (Healthy/MCI/AD)	68/63/89	72/0/77
Post-mortem Interval (years)	7.0 (4.6)	6.6 (6.3)
Education (years)	16.6 (3.4)	-
Tissue Type	DLPFC	Temporal cortex

Table 3
ADNI participant demographics according to disease status

This table includes demographic information for individuals from ADNI included in the imaging GWAS. Values in brackets are standard deviation.

	Healthy Controls (n= 192)	MCI (n=335)	AD (n=79)	*p*-value
*APOE**4 (Carriers/Non-Carriers)	46/146	161/174	56/23	$p = 4.6 \times 10^{-13}$ *
Baseline Age (years)	75.1 (5.2)	72.9 (7.7)	76.6 (7.2)	$p = 0.3$
Education (years)	16.3 (2.7)	16.1(2.7)	14.9 (3.2)	$p = 0.9$
Sex (Female/Male)	78/114	115/220	29/50	$p = 0.35$
PPP4R3A rs2273647 Genotype (C/C, C/T, T/T)	91/81/20	143/151/41	40/30/9	p=0.67

* $p < 0.05$ significant difference in frequencies between groups with Pearson's chi-squared test

MCI= mild cognitive impairment, AD= Alzheimer's disease

Table 4

Demographics for NACC participants (healthy at baseline) according to *PPP4R3A* rs2273647 genotype

This table includes demographic information for individuals from NACC included in the follow-up analyses. Values in brackets are standard deviation.

	T/T (n=130)	C/T (n=381)	C/C (n=359)	*p*-value
*APOE**4 (Carriers/Non-Carriers)	36/94	111/270	97/262	$p = 0.81$
Baseline Age (years)	74.6 (8.8)	74.9 (8.8)	75.1(8.7)	$p = 0.54$
Education (years)	16.6 (7.8)	16 .8(8.9)	16.8 (9.2)	$p = 0.81$
Sex (Female/Male)	68/62	237/144	210/149	$p = 0.47$

Table 5

Demographics for Mayo RNA-Seq data from temporal cortex stratified by disease

There were no significant differences between groups in any of the variables other than *APOE**4 status. Healthy controls had a significantly different proportion of *APOE**4 carriers than AD cases (*$p = 7.5 \times 10^{-7}$, Pearson's chi-squared test). Values with brackets are standard deviation.

	Alzheimer's disease (n=77)	**Healthy Controls (n=72)**
*APOE**4 (Carriers/Non-Carriers)	40/37	9/63*
Age at Death (years)	80.2(7.5)	80.3(8.2)
Sex (Female/Male)	47/30	35/37